Journal of Solid State Chemistry 184 (2011) 1090–1095

Contents lists available at ScienceDirect

Journal of Solid State Chemistry

journal homepage: www.elsevier.com/locate/jssc

Hydrothermal synthesis and thermal properties of a novel cubic $ZrW_{1.80}V_{0.20}O_{7.90}$ solid solution

Xi Chen [a,c], Xuebin Deng [a], Hui Ma [a], Juzhou Tao [b], Xinhua Zhao [a,*]

[a] College of Chemistry and Analysis and Test Center, Beijing Normal University, Beijing 100875, PR China
[b] Experimental Physics Center, Institute of High Energy Physics, Chinese Academy of Sciences, Beijing 100049, PR China
[c] School of Civil Engineering and Communication, North China University of Water Source and Electric Power, Zhengzhou 450011, PR China

ARTICLE INFO

Article history:
Received 12 December 2010
Received in revised form
10 March 2011
Accepted 11 March 2011
Available online 17 March 2011

Keywords:
Synthesis
Solid solution
Negative thermal expansion

ABSTRACT

Tetragonal $ZrW_{1.80}V_{0.20}O_{6.90}(OH)_{2.00}(H_2O)_{2.00}$ hydrate was prepared using an acidic steam hydrothermal (ASH) method. Thermal dehydration followed by phase transformation of this precursor leads to successful synthesis of a novel W-site low-valent substituted cubic $ZrW_{1.80}V_{0.20}O_{7.90}$ solid solution, the mechanism of this process is studied in detail revealing the hydrate and a metastable orthorhombic phase of V'_Wsubstitution solid solution as important intermediate product. This material is found to possess thermal contraction and order–disorder phase transformation properties similar to that of the cubic ZrW_2O_8.

1. Introduction

Cubic ZrW_2O_8 (*c*-ZrW_2O_8) and related compounds have attracted considerable research attention in lattice dynamics physics, solid oxide chemistry and material fields for the last two decades due to their strong isotropic negative thermal expansion (NTE) at high temperature over a wide temperature range [1]. For material application of *c*-ZrW_2O_8-type solid, it is desirable to alter their order–disorder phase transition temperature [2], increase ionic conductivity [3], enhance their strength of compression [4] and improve thermal stability simultaneously [5]. The main approach toward such material optimization goals is by synthesizing and studying cation substituted $Zr_{1-x}M_xW_{2-y}M'_yO_{8-z}$ solid solution with *c*-ZrW_2O_8 type crystal structure. So far successful substitution of *c*-ZrW_2O_8 focuses on the Zr site [2,6–10] and the substitution of Mo (VI) ion [5,11] for W (VI).

ZrV_2O_7 is another important isotropic NTE material [12–14] with a structure closely related to that of *c*-ZrW_2O_8 and consisting of corner-sharing octahedron and tetrahedron. Employing chemical and structural similarities between ZrW_2O_8 and ZrV_2O_7, the first aliovalent substituted cubic solid solution β-$ZrW_{1.8}V_{0.2}O_{7.9}$ was successfully synthesized by a precursor transition method, and its refined structure of a disordered crystal reported recently [15].

Direct synthesis of $ZrW_{1.8}V_{0.2}O_{7.9}$ by solid state reaction has not been achieved so far simply because vanadium oxide sublimes at the high temperature range, where ZrW_2O_8 forms. It is therefore of interest to study the reaction mechanism of this precursor route, through which $ZrW_{1.8}V_{0.2}O_{7.9}$ was successfully prepared.

In this work, dehydration and phase transformation mechanism of such an acidic steam hydrothermal–thermal dehydrating precursor process (ASH–TDP) for preparing aliovalent substituted cubic-$ZrW_{1.80}V_{0.20}O_{7.90}$ was investigated using XRD, TG–DSC–QMS and Raman spectroscopy methods. The properties of ordered α-$ZrW_{1.80}V_{0.20}O_{7.90}$ solid solution were also studied.

2. Experimental section

2.1. Synthesis of hydrated precursor and cubic $ZrW_{2.00-x}V_xO_{8.00-x/2}$ ($x=0$, 0.20) solid solution

The hydrated tetragonal precursors (denoted as HT-precursors) as well as byproduct NH_4Cl were first obtained through an ASH route at 473 K for 24 h as described in Refs. [15,16], using AR grade $ZrOCl_2\cdot 8H_2O$, $(NH_4)_6W_7O_{24}\cdot 6H_2O$ and NH_4VO_3 as reactants. Residual solution after the ASH process was examined for dissolved metal contents by ICP–AES (inductively coupled plasma torch, JY, VITIMA, France) spectroscopy.

On heating HT-precursor to 873 and 813 K for 2 h, respectively, NH_4Cl was decomposed and single phase *c*-$ZrW_{2.00}O_{8.00}$ and $ZrW_{1.80}V_{0.20}O_{7.90}$ were produced.

To avoid interference of NH_4Cl in studying the HT-precursor thermal dehydration mechanism, pure HT-precursors

* Corresponding author. Fax: +86 10 5880 2075.
E-mail addresses: taoj@ihep.ac.cn (J. Tao), xinhuaz@bnu.edu.cn (X. Zhao).

0022-4596/$ - see front matter © 2011 Elsevier Inc. All rights reserved.
doi:10.1016/j.jssc.2011.03.021

$ZrW_{2.00}O_{7.00}(OH)_{2.00}\cdot(H_2O)_{2.00}$ and $ZrW_{1.80}V_{0.20}O_{6.90}(OH)_{2.00}\cdot(H_2O)_{2.00}$ were prepared by re-hydration of cubic $ZrW_{2.00}O_{8.00}$ and $ZrW_{1.80}V_{0.20}O_{7.90}$ using 20 mL of 10 mol L^{-1} as the acidic steam source three times. Unsaturated tetragonal hydrated $ZrW_{1.80}V_{0.20}O_{6.90}(OH)_{2.00}(H_2O)_{2.00-\delta}$ was prepared similarly using 8 mol L^{-1} HNO_3 as the acidic steam source.

2.0000 g HT-precursors of samples were heated at 500 K until the weight remains constant for accurate weight loss measurements.

2.2. Measurement and characterization

All X-ray diffraction (XRD) patterns were collected on a Philips X'Pert MPD diffractometer with X'Celerator detector using Cu-$K\alpha$ radiation. The XRD data were collected from 10° to 120° (2θ) at 0.0167° (2θ) step size and 20 s step time. For phase identification XRD data were collected from 10° to 70° (2θ) and 10 s step time, and the data were indexed using PowderX program [17]. The precise lattice parameters at room temperature were calculated from XRD data calibrated with a SiO_2 internal standard (JCPDS-PDF: 33-1161, Quartz) using the Unitcell software [18].

In situ variable temperature XRD experiments were performed between room temperature to 573 K under flowing nitrogen gas using an Anton Paar TCU 2000 Temperature Control Unit, with sample mounted in an Anton Paar HTK 16 High-Temperature Chamber. Before data collection at each temperature, 3 min interval was kept to make sample achieve thermal equilibrium. Temperature monitoring of all XRD measurements were calibrated by KCl [19] as internal standard.

Quantitative Phase Analysis of polycrystalline materials using X-ray powder diffraction combining Rietveld and Reference Intensity Ratio (Rietveld-RIR QPA) analyses was performed to detect amount of amorphous phase in the ASH products. 0.20 g KCl as an internal standard was added to 2.02 g products. The crystalline phase fractions of the mixture were refined using GSAS software [20]. The crystal structure models used in Rietveld-RIR QPA refer to Ref. [19,21] for KCl and $ZrW_{2-x}V_xO_{7-x/2}(OH)_{2.00}\cdot(H_2O)_{2.00}$, respectively.

Linear dimension change of ceramic pellet with temperature was measured along the pellet diametrical direction by thermal mechanical analysis (TMA Q400, TA-Instruments). The data were collected at a heating rate of 3 K/min from room temperature to 523 K under a constant force of 0.1 N. The peak temperature of TMA curve was calibrated with Al cylinder standard and accurate to ±1 K. The TMA data were analyzed by the TA Universal Analysis software [22].

Differential Scanning Calorimetry–Thermal Gravimetric Analysis–Quadruple Mass Spectrometry (DSC–TGA–QMS) measurement was performed at a heating rate of 30 K/min using STA 449C/QMS 403C (Netzsch) under nitrogen gas flow.

Quantitative IR-spectra were measured on a Nicolet Avatar 360 FTIR Spectrometer (400–4000 cm^{-1}, 4 cm^{-1} resolution, 128 scans) using the KBr pellet technique. 6.00 mg sample and 200.00 mg KBr were mixed and pressed into sample—KBr pellet. All pellets were dried at 313 K for 30 min under IR lamp to reduce the amount of absorbed water in crystal below 2 wt%.

Raman spectra were recorded with a Renishaw inVia Plus spectrometer in the 100–4000 cm^{-1} range with a scan time 10 s. The 514.5 nm line of an Argon ion laser was used as the excitation source. Powder sample data in variable temperature were collected at 293, 303, 323, 353, 373, 393, 423, 443, 473, 493, 513, 533, 553 and 573 K at a heating rate of 30 K/min and a thermal equilibrium interval of 5 min.

3. Results and discussions

3.1. Characterization of the HT-precursors

The ICP–AES measurements indicate that relative amount of Zr, W, V elements dissolved in residual solution after the ASH process is less than 0.1 mol%, confirming no significant loss of metals in the ASH process. XRD patterns of the HT-precursors were indexed consistently to that of tetragonal $ZrMo_2O_7(OH)_2\cdot(H_2O)_2$ (S.G: $I4_1cd$) as shown in Fig. 1. The lattice parameters are $a=11.4375(1)$ Å, $c=12.4950(2)$ Å and $a=11.4371(2)$ Å, $c=12.4810(5)$ Å for precursors of c-ZrW_2O_8 and $ZrW_{1.8}V_{0.2}O_{7.9}$, respectively, which is close to $a=11.45$ Å, $c=12.49$ Å of $ZrMo_2O_7(OH)_2\cdot(H_2O)_2$ [21].

The amounts of amorphous phase is converge to 0.2(3)% and 0.1(2)% for the samples of $ZrW_{2.00-x}V_xO_{7.00-x/2}(OH)_{2.00}(H_2O)_{2.00}$ ($x=0$, 0.20) in the Rietveld-RIR QPA refinements, respectively. Gualtieri et al. indicated that the accuracy of amorphous phase in the sample was determined with absolute error close to 1 wt% when 10 wt% standard is added by using the Rietveld-RIR QPA method [23]. It is rational to believe that the actual amounts of amorphous phase are less than about 1 wt% although the refined results may be underestimation of the amorphous fraction. These results confirm HT-precursors are crystallite products with the targeted compositions. The details of Rietveld-RIR QPA refinement are shown in Appendix A (Supporting Information I).

Accurate measurements of weight loss after heating HT-precursors above their dehydration temperatures until constant weight are 8.40 ± 0.03 wt% (theoretical: 8.43%) and 8.80 ± 0.02 wt% (8.81%) for $ZrW_{2.00-y}V_yO_{7.00-y/2}(OH)_{2.00}(H_2O)_{2.00}$ ($y=0$ and 0.20), respectively. The weight loss of dehydration process corresponds to the following Eq. (1):

$$ZrW_{2.00-y}V_yO_{7.00-y/2}(OH)_{2.00}(H_2O)_{2.00} = ZrW_{2.00-y}V_yO_{8.00-y/2} + 3.00H_2O \ (y=0,\ 0.20) \quad (1)$$

$ZrW_2O_7(OH)_2(H_2O)_2$ is a heterogeneous isomorphism of $ZrMo_2O_7(OH)_2(H_2O)_2$ [24] and has similar atomic coordination. Its structure resembles that of $ZrMo_2O_7(OH)_2(H_2O)_2$ and is a three-dimensional rigid network composed of $[ZrO_3(OH)_2O_2]$-pentagonal bi-pyramid and distorted $[WO_4(OH)(H_2O)]$ octahedron chains cross-linked through oxygen atoms [21]. In order to reveal the configuration of V substitution in structure, Raman spectra of both $ZrW_{1.80}V_{0.20}O_{6.90}(OH)_{2.00}(H_2O)_{2.00}$ and $ZrW_2O_7(OH)_2(H_2O)_2$ were measured and compared as shown in Fig. 2. Based on an empirical relationship established by Hardcastle and Wachs [25] relevant

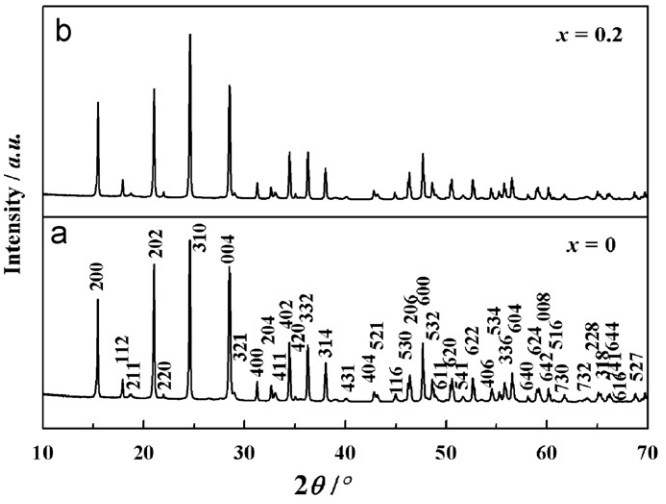

Fig. 1. Indexed XRD patterns of $ZrW_{2.00-y}V_yO_{7.00-y/2}(OH)_{2.00}(H_2O)_{2.00}$ ($y=0$, 0.20).